Supplementary Material to the article "Coherent sub-terahertz frequency phonons in InAs/GaSb superlattices"

1. X-ray Structural Analysis of the Superlattices

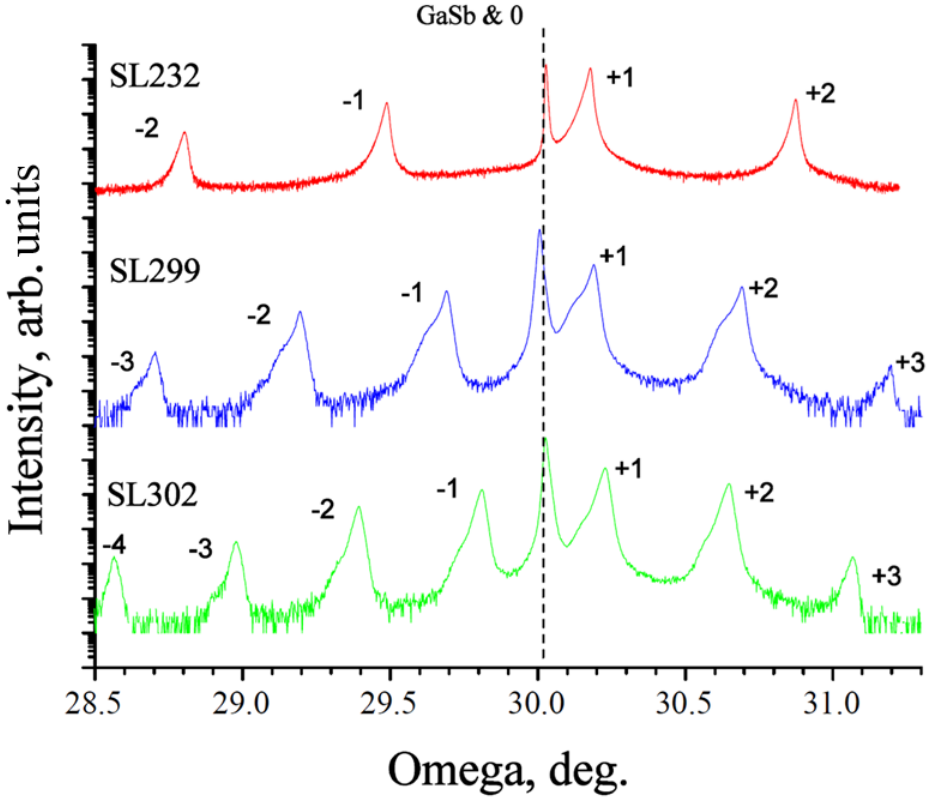

Fig. S1. Rocking curves of the (004) reflection for SL samples SL232, SL299 and SL302.

The data presented in fig. S1 can be used to calculate the period of the superlattice (SL):

$$l = \frac{(n_i - n_i)\lambda}{2(\sin(\theta_i) - \sin(\theta_j))}$$

where l is the period of the InAs/GaSb SL, λ = 1.54178 Å, n_i, n_j are the satellite order numbers, and θ_i, θ_j are the diffraction angles for the corresponding satellites. Obviously, the presence of higher-order diffraction satellites allows for a more accurate calculation of the SL period. The calculation results are shown in Table. 1 of the manuscript. The error in determining the period by this method is at the level of 0.01 nm.

2. Schematic setup

The schematic setup for pump-probe studies under linear polarization is shown in fig. S2. The polarization of the pump and probe radiation was controlled using λ/2 phase plates installed before the final dichroic mirror (DM) near the microscope objective (O).

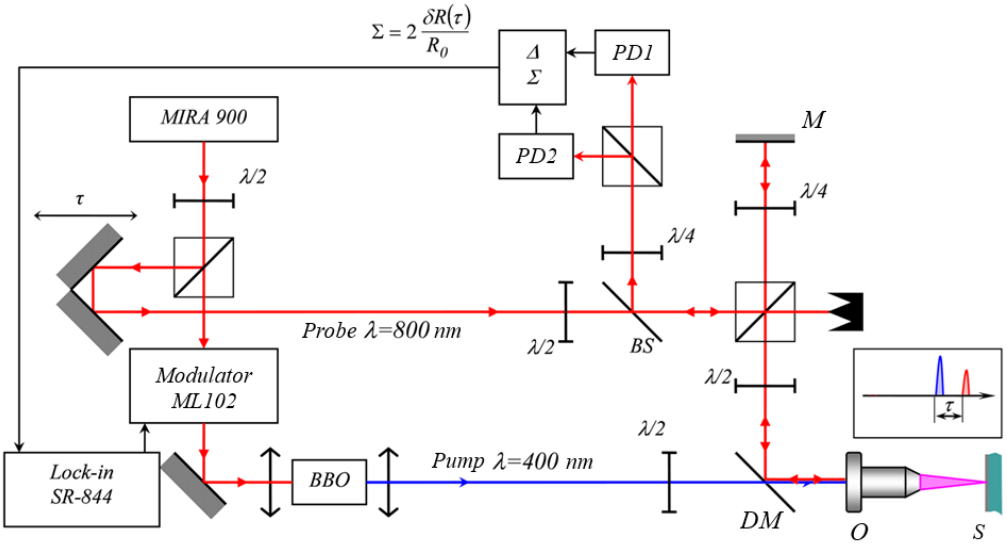

Fig. S2. Experimental setup for linear polarization measurements.

3. Response Analysis

The signal measured consists of three components: i) a sharp peak caused by photoexcited hot carriers; ii) a slower decay caused by cooling of the phonon system heated by hot carriers; and iii) an oscillatory component. A typical raw response for SL232 is shown in fig. S3. The slow component of the response was approximated by the sum of two exponents (red line). Then, to isolate the oscillatory component, the calculated approximation was subtracted from the original response.

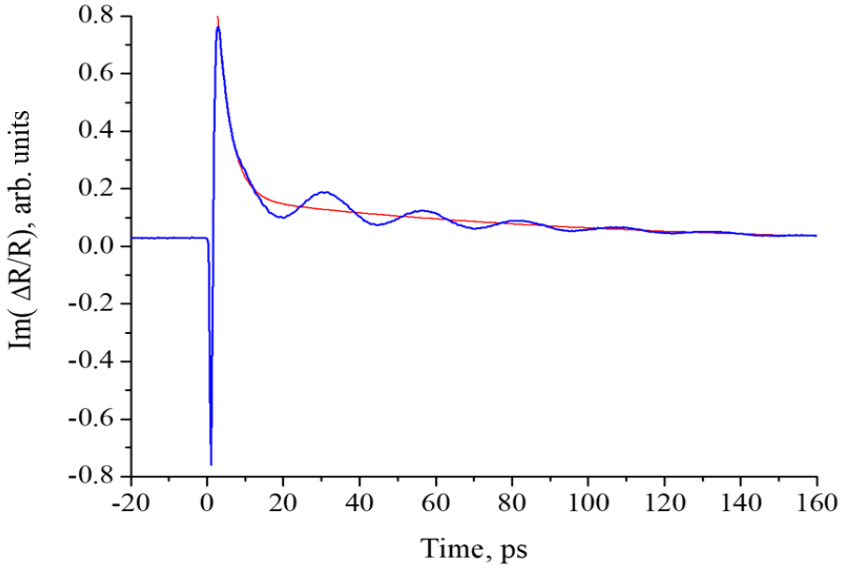

Fig. S3. Original response for SL232 (blue curve) and approximation its slow component.

The result of this subtraction is an oscillatory component with a characteristic shape, shown in fig. 3a of the main text of the article. It consists of damped oscillations with a frequency of ~40 GHz, arising from Mandelstam-Brillouin scattering by an elastic pulse propagating deep into the

sample. The damping is caused by the attenuation of light intensity with depth, and the characteristic decay time is determined by the propagation velocity of the elastic pulse. It is also evident that higher-frequency but weaker oscillations arise against the background of Brillouin oscillations. To isolate them, frequency filtering of the response in the range of 0-220 GHz was performed. The resulting signal is shown in fig. 3b of the main text. Its spectrum and characteristic decay time can also be determined. The resulting spectra of the Brillouin oscillations and the high-frequency component are shown in fig. 3c. A similar procedure was performed for all responses.

It should be noted that, as can be seen from fig. 3, the magnitude of the slow part of the response is several times greater than the low-frequency oscillating part, and the magnitude of the rapidly varying part, due to the properties of the SL, is 1-2 orders of magnitude smaller (see fig. 3 of the main text).

4. Dispersion and Group Velocity of Sub-Terahertz Phonons in the Superlattice

InAs and GaSb are characterized by similar values of lattice constant, density (ρ), and elastic tensor components (C_{ij}). This implies that to describe the dispersion $\omega_i^{\bar{g}}(\bar{k})$ of acoustic waves in the SL, it is sufficient to project fragments of the linear frequency dependence on the wave vector $\omega_i(\bar{q}) = v_i^{\bar{q}} \cdot |\bar{q}|$, corresponding to a homogeneous medium with the SL-period-averaged ρ and C_{ij}, into the SL's Brillouin zone: $\omega_i^{\bar{g}}(\bar{k}) = v_i^{\bar{q}} \cdot |\bar{k} + \bar{g}|$. Here, $\omega_i(\bar{q})$ is the frequency of an acoustic wave in a homogeneous medium corresponding to one of the three *(i=1,2,3)* acoustic modes, $\bar{k}$ is the quasivector of the phonon in the SL, $\bar{g}$ is an arbitrary vector of the SL's reciprocal lattice, $\bar{q} = \bar{k} + \bar{g}$ and $v_i^{\bar{q}}$ is the propagation velocity of the *i*-th phonon mode along the direction of vector q.

Each branch of the dispersion curve $\omega_i^{\bar{g}}(\bar{k})$ obtained in this way is indexed by the type of the original oscillation (*i*) and the value of the vector $\bar{g}$. This approach is widely used for describing the dispersion of acoustic phonons in SLs composed of materials with weak contrast in acoustic properties [9]. For describing the sub-terahertz phonons corresponding to the peaks $\Omega^{\pm}$ and Ω^0, the minimal non-trivial magnitude reciprocal lattice vectors $\pm\bar{g}_0(0,0,2\pi/l)$ play a key role.

	$\omega/2\pi$ ex., GHz	v_l^{001}, m/s	$\lambda/2n$, nm	$\omega/2\pi$ th., GHz	l, nm	$\Omega^-/2\pi$ th., GHz	$\Omega^-/2\pi$ ex., GHz	$\Omega^+/2\pi$ th., GHz	$\Omega^+/2\pi$ ex., GHz	$\Omega^0/2\pi$ th., GHz	$\Omega^0/2\pi$ ex., GHz
CP232	38.5	3870	100	38.7	7.356	487.5	491	564.5	569	527.5	530
CP299	38.5	3870	100	38.7	10.23	339.9	339	416.9	416	380.4	384
CP302	38.5	3870	100	38.7	12.17	279.4	277	356.4	354	320.3	322

Table S1. Theoretical (th.) spectral positions of the peaks $\omega/2\pi$, $\Omega^{\pm}/2\pi$, $\Omega^0/2\pi$ based on v_l^{001}, $\lambda/2n$, l and their comparison with experimental (ex.) data presented in table 2 of the main text. The calculation error is noticeably larger than the experimental error, due to the lack of precise data on the refractive index of light in the SL (n) and the sound velocity (v_l^{001}).

The known phonon dispersion in the SL $\omega_i^{\bar{g}}(\bar{k})$ allows us to calculate the group velocity vector for a given phonon mode using the formula $\bar{V}_i^{\bar{g}}(\bar{k}) = \nabla_k \cdot \omega_i^{\bar{g}}(\bar{k})$. For the longitudinal phonons corresponding to the $\Omega^{\pm}$ peaks, the following result is obtained:

$$\bar{V}_i^{\pm\bar{g}_0}(\bar{k}) = v_l^{\bar{k}\pm\bar{g}_0} \begin{pmatrix} k_X/\sqrt{k_X^2 + k_Y^2 + (k_Z \pm 2\pi/l)^2} \\ k_Y/\sqrt{k_X^2 + k_Y^2 + (k_Z \pm 2\pi/l)^2} \\ (k_Z \pm 2\pi/l)/\sqrt{k_X^2 + k_Y^2 + (k_Z \pm 2\pi/l)^2} \end{pmatrix} = v_l^{001} \begin{pmatrix} 0 \\ 0 \\ \pm 1 \end{pmatrix}$$

The validity of the equality on the right side is determined by the fact that for the $\Omega^{\pm}$ phonons, the components $k_x = k_y = 0$. For the phonons corresponding to the Ω^0 peak, the following is obtained:

$$\bar{V}_i^{\bar{g}_0}(\bar{k}) = v_l^{\bar{k}+\bar{g}_0} \begin{pmatrix} k_X/\sqrt{k_X^2 + k_Y^2 + (k_Z \pm 2\pi/l)^2} \\ k_Y/\sqrt{k_X^2 + k_Y^2 + (k_Z \pm 2\pi/l)^2} \\ (k_Z + 2\pi/l)/\sqrt{k_X^2 + k_Y^2 + (k_Z + 2\pi/l)^2} \end{pmatrix} \approx v_l^{001} \begin{pmatrix} k_X/g \\ k_Y/g \\ 1 \end{pmatrix}$$

The validity of the approximate equality on the right-hand side is determined by the fact that for the Ω^0 phonons, the component $k_z = 0$ and components k_x, k_y are on the order of the Brillouin quasivector $4\pi n_X/\lambda$, hence $k_x, k_y \ll 2\pi/l$. One can see that phonons of this type propagate at a small angle of $\sim 2n_X l/\lambda$ to the cleaved surface of the SL.